ANALYSIS OF E-PLANE CIRCULATORS BY EIGENVALUE MEASUREMENTS

U. Goebel and Ch. Schieblich

Technische Universität Hamburg-Harburg, Arbeitsbereich Hochfrequenztechnik,
Postfach 90 14 03, Wallgraben 55, D-2100 Hamburg 90, West-Germany

ABSTRACT

The operation of E-plane waveguide circulators is explained and verified by eigenvalue measurements. Besides the reverse type circulator, which is usually realized but has inherently small bandwidth, a forward type operation has been found with good potentials for broad-band performance. A model at 10 GHz showed 20 % bandwidth at 20 dB isolation without using external transformers.

INTRODUCTION

In the last years, integration of several waveguide and fin-line devices in E-plane geometry has found growing interest for the mm-wave range. Hence circulators in E-plane geometry became important. Unfortunately, the performance of the common E-plane circulator is mostly inferior to H-plane circulators, because it operates as reverse type /1/. By means of a recently developed network analyzer system /2/, various configurations of E-plane circulators could be studied. The most remarkable result is the realization of E-plane forward type circulators, which operate below both split frequencies of the circularly polarized eigenmodes. As forward type circulators, they show improved broadband capability.

THE MEASURING SYSTEM

For the analysis of a circulator, the scattering matrix or its eigenvalues must be known in magnitude and phase. Since direct vector measurement of the transmission parameters is cumbersome and requires extensive RF-switching, we developed another method /2/, which uses the capabilities of a minicomputer controling both a vector network analyzer (HP 8410C) and a scalar analyzer (PM 1038). The fundamental idea is to measure the input reflection coefficient of the circulator with 3 sets of terminations (for example as in fig. 1). If ports 2 and 3 of the circulator are terminated by the reflections Γ_2 and Γ_3, the input reflection reads

$$\Gamma_{in} = S_{11} + \frac{(\Gamma_2+\Gamma_3)A + \Gamma_2\Gamma_3(B-2S_{11}A)}{1 - (\Gamma_2+\Gamma_3)S_{11} + \Gamma_2\Gamma_3(S_{11}^2-A)} \qquad (1)$$

$$A = S_{12}\cdot S_{13}\,, \qquad B = S_{12}^3 + S_{13}^3.$$

With three sets of terminations we get a set of linear equations that can be solved for S_{11}, A, B. Then S_{12} and S_{13} are given by

$$\left.\begin{matrix} S_{12}^3 \\ S_{13}^3 \end{matrix}\right\} = \frac{B}{2} \pm \sqrt{\left(\frac{B}{2}\right)^2 - A^3}\,, \qquad S_{12} = \frac{A}{S_{13}} \qquad (2)$$

One cannot distinguish between S_{12} and S_{13} from one-port measurements alone. The missing information can, however, be taken from the scalar measurement. The phases of S_{12} and S_{13} are unique except for multiples of 120°. For weakly nonreciprocal junctions ($S_{12} \approx S_{13}$) the difference in the root of equ. (2) becomes small, leading to an untolerable amplification of measurement errors. In this case the evaluation algorithm uses the transmission magnitudes obtained with a scalar detector at port 3 of the circulator with terminations a) and b) of fig. 1.

The complete measurement system is shown in fig. 2. The RF part consists of standard waveguide and/or coaxial components. Reflection and both transmission magnitudes can be measured online. Reflection coefficient measurements are corrected by an 8-term error model, nonlinearity of the scalar network-analyzer and mismatch of the 10 dB-attenuators are canceled by appropriate calibration procedures. At least three measurement cycles are necessary (load/load; load/short; short/short). The short-circuits in the reference plane are realized by movable backshort plates across the waveguide. The data can then be processed and displayed in various ways, e.g. conversion between S-parameters and eigenvalues or shifting the reference plane is possible.

Fig. 3 shows a sketch of the waveguide housing used in the experiments. The feeding waveguides (22.86 × 10.16 mm) are tapered to half height to allow small junction diameters. The junction height can be adjusted by two plungers, which contact the side walls.

REVERSE TYPE OPERATION

It is very advantageous to describe a circulator in terms of its scattering matrix eigenvalues, since the interaction between incident fields and the individual junction/ferrite modes can be read directly from the eigenvalue phases. All measurements were taken with respect to a reference plane that coincides with the junction axis. The empty E-plane junction approximates a series junction, which has the eigenvalues $s_0 = -1$ and $s_+ = s_- = 1$ /1/. Fig. 4a shows the corresponding measurement. The

0149-645X/86/0000-0257$01.00 © 1986 IEEE

deviation of the s_o-phase from 180° is caused by the finite extension of the junction, which can be understood as a radial two-plate line with different propagation constants for different angular dependences.

A ferrite disc at one or both ends of the junction exhibits series resonant behaviour as stated in /3/. The lowest resonance is the $E_{11\delta}$, an angle-dependent mode, which responds only to rotating eigenexcitations. Fig. 4b shows the corresponding measurement. Splitting this resonance by a magnetic bias field results in reverse type circulation (Fig. 4c-d) which has been discussed in /1/.

FORWARD TYPE OPERATION

In /1/, it has been shown that reverse type circulators are inherently smaller-banded than forward type circulators, because a larger phase shift of the rotating eigenvalues is required to establish circulation conditions. So we aimed to realize a forward type circulator in E-plane geometry. The lower rudimental counter-circulating band of the reverse type circulator serves as a starting point. To achieve forward type circulation, the unmagnetized junction must meet the following conditions:

1. The eigenvalues s_o and s_+/s_- must have opposite phase.
2. The incident fields corresponding to s_+/s_- have to be influenced by an angular dependent ferrite mode.

The junction of fig. 4 meets the second condition in the vicinity of resonance. The first condition is met elsewhere, but without ferrite interaction.

An increased coupling to the $E_{11\delta}$-mode leads to a broadband negative phase shift below its resonance. This must be compensated by an additional positive phase shift to maintain condition 1.

Both can be achieved by reducing the height of the junction, which raises its cutoff frequency. Hence the wavelength becomes larger, resulting in a positive phase shift. Furthermore, an impedance transformation to a lower level is introduced at the plunger edges, which leads to a much stronger coupling. The in-phase eigenvalue remains nearly unaffected, because it is a short circuit in the junction axis. Due to the small junction diameter this approaches the limiting case with a junction height of zero. Fig. 5 shows the situation with a junction height reduced by 22 %, yielding a cutoff frequency of about 8.3 GHz. Only one of the plungers is inserted. When the ferrite of fig. 4 is attached to the inserted plunger, we get the eigenvalue diagram of fig. 5. The $E_{11\delta}$-resonance is shifted to a higher frequency (about 12.6 GHz); this is an effect of the reduced junction height. In contrary to fig. 4 we now observe broadband interaction between the ferrite and s_+, s_-. When bias field is applied, the $E_{-11\delta}$-mode is shifted down, the $E_{+11\delta}$-mode up (Fig. 5c). Forward type circulation occurs at about 10.75 GHz, where the eigenvalue phases are 120° apart.

Up to now, the performance is not satisfying. This is due to the almost non-dispersive s_o (Fig. 5a-c), while the paths of s_+ and s_- indicate that this structure has broadband capability.

Dispersion for s_o can be introduced by lowering the resonant frequency of the first in-phase mode, namely the H_{011} of the resonator established by the two plungers and the junction sidewalls with respect to the $E_{11\delta}$-mode of the ferrite. This can be done by introducing symmetry with respect to the halving plane, i.e. two equal ferrite discs. The so established magnetically conducting wall raises the $E_{11\delta}$ resonance frequency. The s_+/s_- resonance frequency can be retained by bigger ferrites, simultaneously lowering the H_{011} resonance frequency. The latter causes a parallel resonance at 13.5 GHz (Fig. 6a). In the magnetized junction, the circulation band is limited by a reverse type circulation above 11.6 GHz (Fig. 6c). The eigenvalue diagram fig. 6b shows that this is caused by an in-phase resonance, namely the H_{011}-mode, which is tuned down by the bias field. (The μ_z component of the permeability tensor of the unmagnetized ferrite is less than one and approaches unity above saturation /4/). At the lower edge, circulation bandwidth is limited by a deviation in the s_+-phase, probably due to the step discontinuity at the plunger edges.

It is remarkable that the operating band of the forward type E-plane circulator is located below the resonance frequencies of both rotating eigenexcitations, i.e. the circulator works with relatively small ferrites. Probably, the E-plane circulator presented in /5/ works similar. The ferrite dimensions there are also relatively small and match the scaled dimensions of our ferrite.

ACKNOWLEDGEMENT

The authors wish to thank the Deutsche Forschungsgemeinschaft for financial support.

REFERENCES

/1/ U. Goebel, Ch. Schieblich: "A Unified Equivalent Circuit Representation for H- and E-plane Junction Circulators", EuMC 1983, pp.803-808.

/2/ Ch. Schieblich, U. Goebel: "Complete Determination of Circulator Eigenvalues without Transmission Phase Measurement", MTT-S Symposium Digest 1985, pp. 489-492.

/3/ K. Solbach: "Equivalent Circuit Representation for the E-plane Circulator", IEEE Trans. MTT-30, 1982, pp. 806-809.

/4/ J. Green, F. Sandy: "Microwave Characterization of Partially Magnetized Ferrites", IEEE Trans. MTT-22, 1974, pp. 641-651.

/5/ M. Omori: "An Improved E-plane Waveguide Circulator", IEEE G-MTT Int. Microwave Symp., 1968, pp. 228-236.

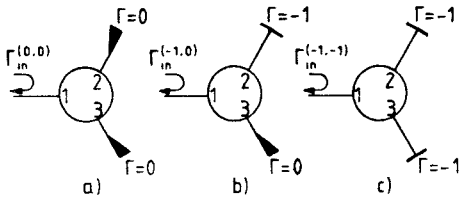

Fig.1: Circuits for the three reflection coefficient measurements

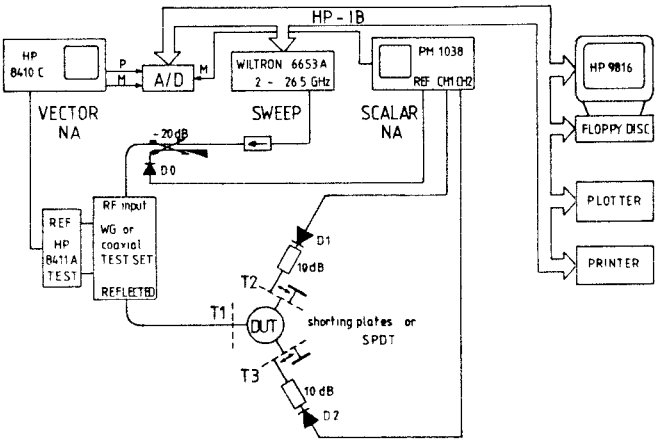

Fig.2: The complete analyzer system

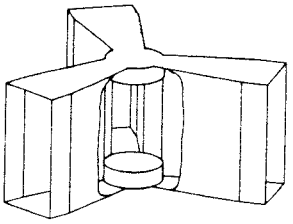

Fig.3: The experimental E-plane circulator

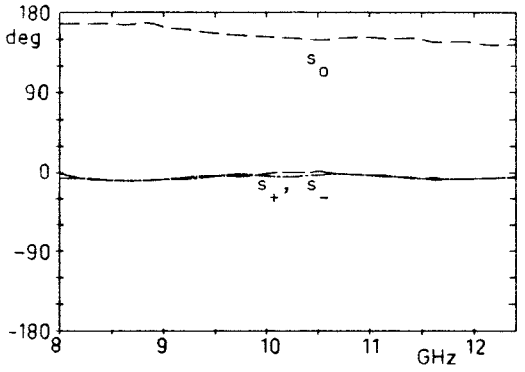

a) Eigenvalues without ferrite

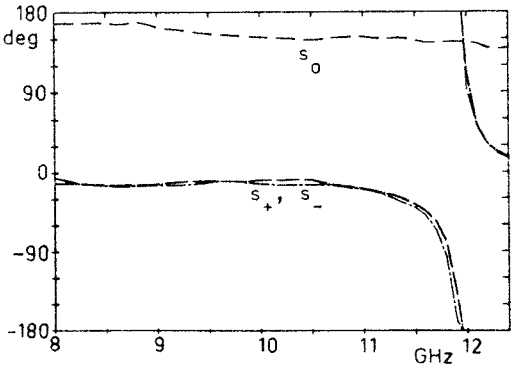

b) Eigenvalues with unmagnetized ferrite

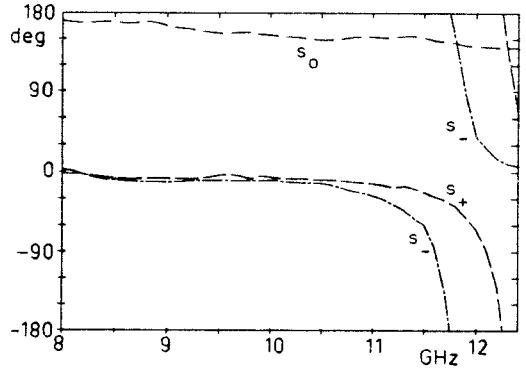

c) Eigenvalues with magnetized ferrite

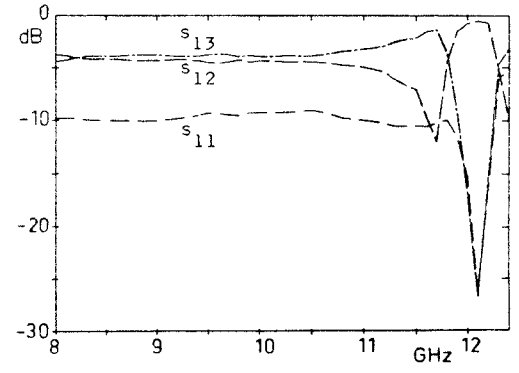

d) Scattering parameters with magnetized ferrite

Fig.4: Junction without plungers, one ferrite disc 6 Ø x 4 mm RF 2 (Telefunken)

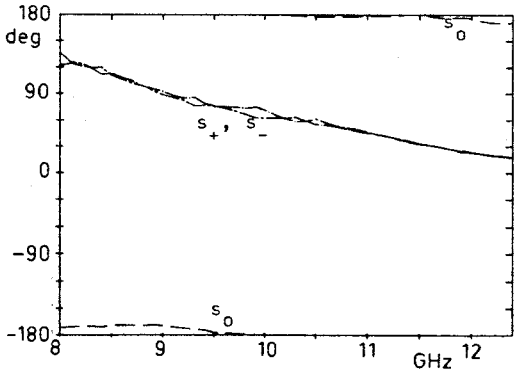

a) Eigenvalues without ferrite

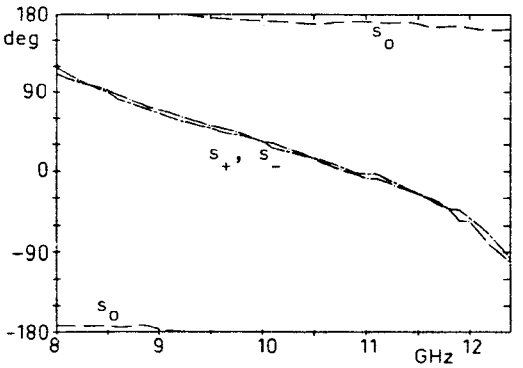

b) Eigenvalues with unmagnetized ferrite

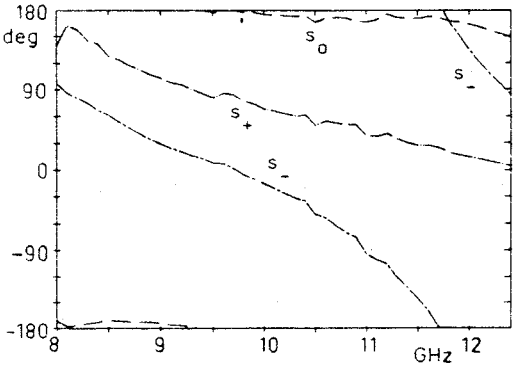

c) Eigenvalues with magnetized ferrite

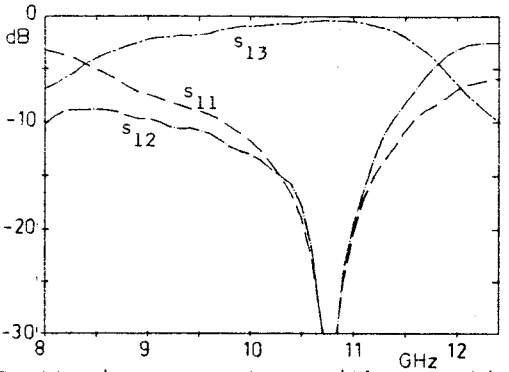

d) Scattering parameters with magnetized ferrite

Fig.5: Junction with one plunger 9 Ø x 6 mm, one ferrite disc 6 Ø x 4 mm RF 2

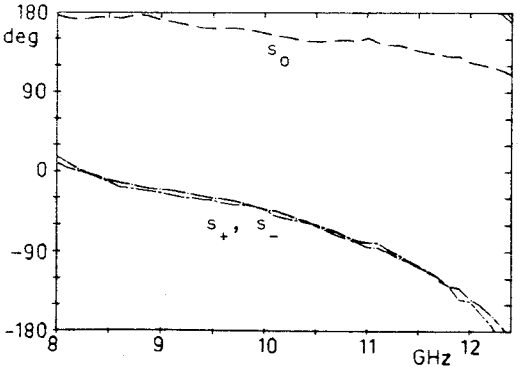

a) Eigenvalues with unmagnetized ferrites

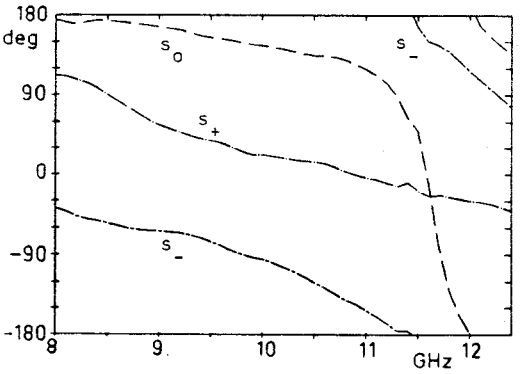

b) Eigenvalues with magnetized ferrites

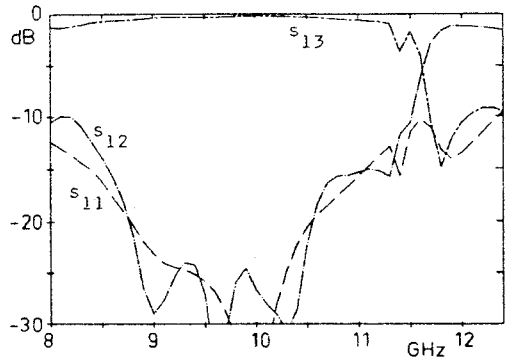

c) Scattering parameters with magnetized ferrites

Fig.6: Junction with two plungers
9 Ø x 2.5 mm, two ferrite discs
6.5 Ø x 5 mm RF 2